a definitive description of all the structural features of butyl rubber, including those of the isoprenyl residues.

Acknowledgment. We express our gratitude to Dr. G. J. Wilson for useful discussions and to Polysar Ltd. for permission to publish this work.

Registry No. (*Z*)-**2**, 96292-80-7; (*E*)-**2**, 96292-81-8.

References and Notes

(1) J. P. Kennedy and I. Kirschenbaum, *High Polym.*, **24**, 691 (1969).
(2) J. Rehner, Jr., *Ind. Eng. Chem.*, **36**, 46 (1944).
(3) F. P. Baldwin and R. H. Schatz, "Kirk-Othmer Encyclopedia of Chemical Technology", 3rd ed., Wiley-Interscience, New York, 1979, Vol. 8, p 470.
(4) H. Yu Chen and J. E. Field, *J. Polym. Sci., Part B*, **5**, 501 (1967).
(5) A. Van Tongerloo and R. Yukov, *Proc. Int. Rubber Conf., Venice*, 70 (1979).
(6) C. Corno, A. Proni, A. Priola, and S. Cesca, *Macromolecules*, **12**, 411 (1979).
(7) R. Vukov, *Rubber Chem. Technol.*, **57**, 275 (1984).
(8) M. A. Golub, S. A. Fuqua, and N. S. Bhacca, *J. Am. Chem. Soc.*, **84**, 4981 (1962).
(9) A. G. Evans and G. W. Meadows, *Trans. Faraday Soc.*, **46**, 327 (1950).
(10) D. M. Grant and E. G. Paul, *J. Am. Chem. Soc.*, **86**, 2984 (1964).
(11) M. Malanga and O. Vogl, *J. Polym. Sci., Polym. Chem. Ed.*, **21**, 2629 (1983).
(12) L. P. Lindeman and J. Q. Adams, *Anal. Chem.*, **43**, 1245 (1971).
(13) D. H. Beebe, *Polymer*, **19**, 231 (1978).

Dynamics of Cubic Lattice Models of Polymer Chains at High Concentrations

Charles C. Crabb† and Jeffrey Kovac*

Department of Chemistry, University of Tennessee, Knoxville, Tennessee 37996-1600.
Received October 29, 1985

ABSTRACT: The dynamics of cubic lattice models of polymer chains are studied over a wide range of concentration by means of computer simulation. Three dynamic properties—the terminal relaxation time, the center of mass diffusion constant, and the central monomer diffusion—were studied. All three properties show clear deviations from the Rouse theory at high concentrations, but do not conform to the predictions of the reptation model.

Introduction

The dynamics of linear polymers are ordinarily discussed in terms of two models which are supposed to describe the motions of chains at the two extremes of behavior. In dilute solution the dynamics are reasonably well described by the venerable Rouse–Zimm model and its modifications.[1] The Rouse–Zimm model, however, assumes an ideal, phantom chain so neither the static nor dynamic effects of excluded volume can easily be incorporated. At the other extreme of long chains in bulk polymers the reptation model of DeGennes is ordinarily used.[2,3] The reptation model assumes that the motion of the chain is completely dominated by intermolecular entanglements so that the chain must diffuse along its contour in a snakelike fashion.

The reptation concept has been extremely fruitful. It has been elaborated into a complete theory of polymer melts by Doi and Edwards[4] and applied to a number of other problems including polymer crystallization,[5] crack healing,[6] and the Tromsdorff effect.[7] Graessley[8] has recently surveyed the theories and experimental data relevant to the reptation and Doi–Edwards theory and found qualitative agreement. DeGennes and Leger[9] have reviewed microscopic experimental probes of the reptation model and found that the data, on the whole, support the theory.

Despite the successes of the reptation model it remains controversial. Dynamic neutron scattering experiments have failed to see any evidence of reptation.[10] Computer simulation studies designed to study entanglement effects have generally failed to see reptation except in systems where a single chain is allowed to move among frozen chains or fixed obstacles.[11–15] Some of these computer studies are flawed, but the recent simulation of diamond lattice chains by Kremer[15] studied a system whose static properties indicated that it was well into the entanglement region, but the dynamic properties showed no sign of reptation. DeGennes and Leger[9] have argued that the dynamic neutron scattering studies are not able to probe a sufficiently large length scale. They have also suggested that computer simulations cannot study chains long enough to see reptation with present-day computers. At this time it seems that the question of the regime of validity of the reptation model is still unresolved.

Even if the reptation model is correct for the extreme cases of very long chains at high concentrations, chains in glassy systems, and chains trapped in networks, there is still a wide range of concentrations and chain lengths where the chain dynamics are affected by entanglements, but where the results of the reptation theory are not valid. Since there is no general theory of entanglement effects, computer simulation studies can play an important role in increasing our understanding of these effects. In this paper we report the results of an extensive computer simulation study of cubic lattice chains. Chains of lengths 12, 24, and 48 have been studied at concentrations varying from $c = 0$ (isolated chains) to $c = 0.90$. The equilibrium mean square end-to-end distance, $\langle R^2 \rangle$, and three dynamic properties—the terminal relaxation time, the center of mass diffusion constant, and the diffusion of a central monomer—have been computed. The focus has been on the chain length dependence of scaling behavior of the terminal relaxation time and the center of mass diffusion constant, and how the scaling behavior changes with concentration. We have also studied the concentration and chain length dependence of the central monomer diffusion. The central questions that we tried to answer were these: At what concentrations (if any) do deviations from the

† Present address: Rohm and Haas Research Laboratories, Rohm and Haas Co., Bristol, PA 19007.

0024-9297/85/2218-1430$01.50/0

predictions of the Rouse model occur and to what extent do those deviations conform to the predictions of the reptation model?

Model

The model used in the simulations is the straightforward extension to a multiple-chain system of the model used by Gurler, Crabb, Dahlin, and Kovac[16] to study the dynamics of single chains in the presence of excluded volume. n identical chains each consisting of N beads ($N - 1$ steps) are placed on a cubic lattice. Periodic boundary conditions are employed. The periodic box is large enough ($20 \times 20 \times 20$) that self-entanglements due to the chain "wrapping around the box" are avoided. The excluded volume condition is rigorously observed for both intramolecular and intermolecular contacts. In the movement algorithm first a chain is chosen at random and then a bead on the chain is chosen at random. Depending on the local conformation surrounding a bead, one of the elementary chain motions is attempted. Each attempted move is called a bead cycle. The end-bead, normal-bead, and 90° crankshaft motions are the three elementary motions employed. The model is discussed in detail in our previous paper.[16]

All simulation runs were begun from a fully equilibrated configuration as determined by monitoring the mean square end-to-end distant $\langle R^2 \rangle$ and the center of mass position of several selected chains. Equilibrium was assumed when two conditions were fulfilled. First, the value of $\langle R^2 \rangle$ had to be essentially constant for an extended period. Second, the center of mass of the selected chains had to have diffused over a large distance (several times $\langle R^2 \rangle^{1/2}$). We were conservative in judging equilibration and, if there was any doubt, allowed the system to run longer. From time to time the end-to-end vector, $\vec{R}(t)$, the center of mass position, $\vec{C}(t)$, and the position of a central bead (monomer) $\vec{M}(t)$ were sampled. The time unit used throughout is nN bead cycles. As discussed in our previous paper we feel that this is the natural choice for the time unit in simulations of this type.[16] This choice for the time unit allows each bead in the system to move once (on the average) per unit time.

The values of $\vec{R}(t)$ were used to compute the mean square end-to-end distance $\langle R^2 \rangle$ and the end-to-end vector autocorrelation function, $\rho(t)$, defined as

$$\rho(t) = \langle \vec{R}(t) \cdot \vec{R}(0) \rangle / \langle R^2 \rangle \tag{1}$$

The ensemble average was computed as a time average and also averaged over all chains in the system to reduce statistical errors. The terminal relaxation time of the chain, τ, is estimated by fitting a least-squares line to the linear, long-time region of a semilog plot of $\rho(t)$ vs. t. τ is then calculated as the negative inverse of the slope of this line. A better way of calculating this quantity would be to study the relaxation of the Rouse coordinates. A study of the relaxation of the Rouse coordinates of single chains has shown that our previously reported relaxation times for single chains do not differ significantly from those obtained in the more careful normal-coordinate analysis.[17] We are therefore confident that the values of τ reported below are good estimates of the terminal relaxation times of the chains. We do plan to confirm our results by doing the normal-coordinate analysis.

The self-diffusion has been studied by computing the mean square displacement of the center of mass, $\langle (\Delta C)^2 \rangle$, defined as

$$\langle (\Delta C(t))^2 \rangle = \langle (\vec{C}(t) - \vec{C}(0))^2 \rangle \tag{2}$$

The ensemble average is again computed as a time average and also averaged over all chains in the system. The self-diffusion coefficient was estimated by fitting a least-squares line to a plot of $\langle (\Delta C(t))^2 \rangle$ vs. t. The slope of this line is then $6D$, where D is the self-diffusion coefficient.

The third dynamical quantity to be studied was the mean square diffusion of a central monomer $\langle (\Delta M(t))^2 \rangle$ defined as

$$\langle (\Delta M(t))^2 \rangle = \langle (\vec{M}(t) - \vec{M}(0))^2 \rangle \tag{3}$$

The ensemble average was computed as a time average and also averaged over all the chains in the system.

Table I
Mean Square End-to-End Distance ($\langle R^2 \rangle$) as a Function of Chain Length (N) and Concentration (c)

c^a	$\langle R^2 \rangle$ $N = 12$	$N = 24$	$N = 48$	$2\nu^b$
0.000	18.86	46.15	107.99	1.196
0.096	18.50	44.15	101.88	1.175
0.192	18.16	42.66	95.24	1.141
0.288	17.90	41.49	92.85	1.134
0.384	17.57	40.30	88.21	1.111
0.750	16.58	35.97	78.58	1.071
0.900	16.02	35.19	75.97	1.064
second-order random walk	15.875	33.875	69.875	

[a] Units: beads per lattice site. [b] Scaling exponent for the relation $\langle R^2 \rangle \sim N = 1$. The values for the exponents are the slopes of the least-squares lines shown in Figure 1.

Results and Discussion

Monte Carlo simulations were performed for chains of lengths $N = 12$, 24, and 48 at concentrations ranging from $c = 0$ (isolated chain) to $c = 0.900$. The concentration is measured in units of beads per lattice site. The results for the equilibrium dimensions will be discussed briefly before proceeding to the dynamic properties which were the main focus of the work.

Equilibrium Dimensions. Values of the mean square end-to-end distance, $\langle R^2 \rangle$, for the various chain lengths and concentrations are given in Table I. As expected the chain dimensions decrease smoothly with increasing concentration. They appear to be approaching a value slightly larger than the dimensions of a second-order random walk at unit concentration. Figure 1 is a scaling plot of ln $\langle R^2 \rangle$ vs. ln $(N - 1)$. The slopes or scaling exponents decrease from the single-chain, excluded volume value of 1.2 at $c = 0$ to 1.064 at $c = 0.900$. The slope at $c = 0.900$ is fairly close to the ideal chain value of 1.0 and consistent with that obtained in other simulations. Figure 2 is a plot of ln $[\langle R^2 \rangle (N - 1)^{-1}]$ vs. ln c. This figure clearly shows the decrease in chain dimensions with concentration. The values for the second-order random walk have also been plotted at $c = 1.0$. A second-order (or nonreversing) random walk is one in which immediate step reversals are not permitted, but longer range overlaps are allowed.[25] This is the appropriate choice for the $c = 1$ limit in a lattice simulation. The self-reversal excluded volume constraint cannot be screened out in a lattice model even at unit concentration. A line of slope −0.25 is drawn for comparison with the scaling prediction for semidilute solutions.[3] Figure 2 shows that our results for the equilibrium dimensions are consistent with the results of many other simulations as recently summarized and analyzed by Bishop, Kalos, Sokal, and Frisch.[18]

Terminal Relaxation Times. A typical semilog plot of the end-to-end vector autocorrelation function $\rho(t)$ for $N = 24$ and $c = 0.900$ is shown in Figure 3. The autocorrelation functions for all other cases behave similarly. The decay appears to be linear (on the semilog plot) at long times. This indicates that the decay is exponential at long times. The least-squares line used to determine the re-

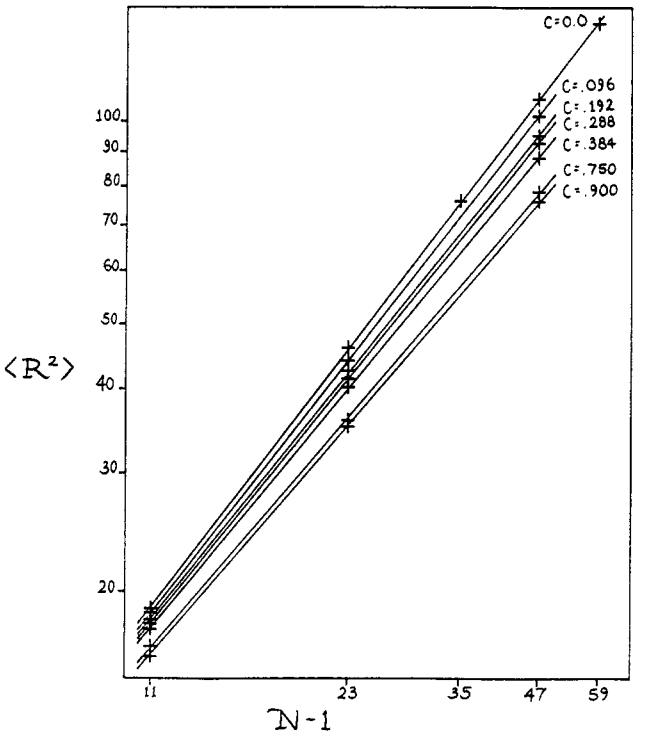

Figure 1. Double logarithmic plot of mean square end-to-end distance, $\langle R^2 \rangle$, vs. chain length, $N-1$, for various concentrations. The solid lines are linear least-squares fits used to determine the scaling exponents.

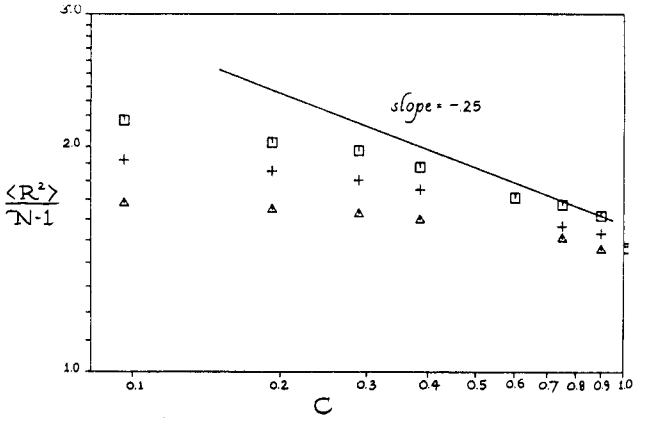

Figure 2. Double logarithmic plot of $\langle R^2 \rangle (N-1)^{-1}$ vs. concentration, c. Values are shown for $N-1 = 11$ (△), $N-1 = 23$ (+), and $N-1 = 47$ (□). The values plotted at $c = 1$ are the dimensions of a second-order random walk as computed from the formula given by Domb.[25] A line of slope −0.25 is also shown for comparison.

laxation time is also shown. In each case the least-squares fit was done over the longest linear region possible which was also linear in almost all plots, chosen "by eye". We tried to be consistent and not change the region of fit unless obvious curvature was observed. Efforts are under way to check these relaxation times by calculating the autocorrelation functions of the normal modes. As mentioned above, a normal-coordinate check of our previously published single-chain relaxation times showed essentially no difference between the two methods.

The values of the relaxation times are collected in Table II. Figure 4 is a scaling plot of ln τ vs. ln $(N-1)$. A least-squares line was fitted to the data to estimate the exponent α in the scaling relationship

$$\tau \sim (N-1)^{\alpha} \tag{4}$$

The slopes or scaling exponents are also given in Table II.

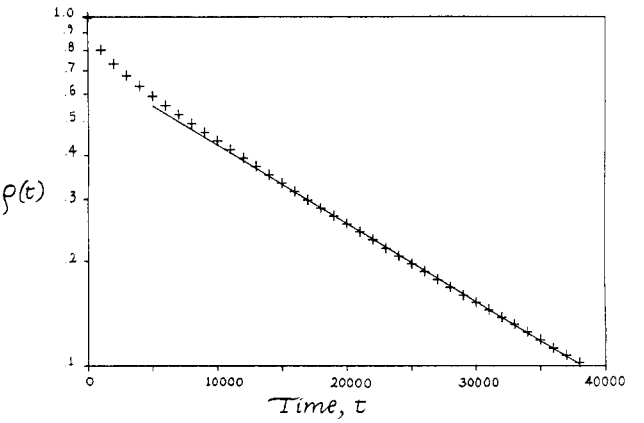

Figure 3. Semilogarithmic plot of the end-to-end vector autocorrelation function, $\rho(t)$, vs. time for chain length $N = 24$ at concentration $c = 0.90$. The time unit is nN bead cycles. The solid line is a linear least-squares fit to the linear long-time region used to estimate the relaxation times.

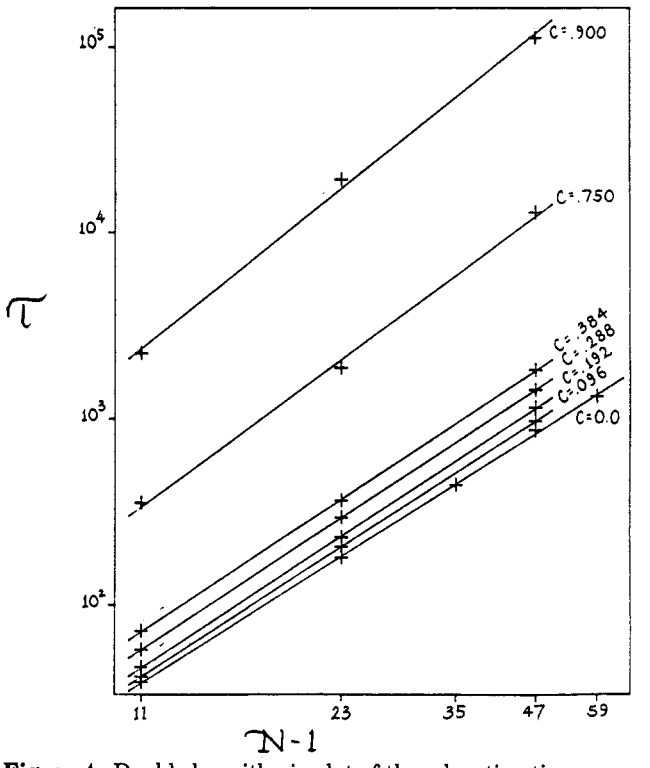

Figure 4. Double logarithmic plot of the relaxation time, τ, vs. chain length, $N-1$, for various concentrations. The solid lines are linear least-squares fits used to determine the scaling exponents, α.

Table II
Terminal Relaxation Times (τ) as a Function of Chain Length (N) and Concentration (c)

	τ			
c^a	$N = 12$	$N = 24$	$N = 48$	α^b
0.000	38.5	179	874	2.13
0.096	41.36	206	978	2.18
0.192	46.40	231	1160	2.21
0.288	57.56	295	1440	2.22
0.384	72.50	366	1840	2.23
0.750	354	1890	12900	2.47
0.900	2240	19400	112000	2.70

[a] Units: beads per lattice site. [b] Scaling exponent for the relation $\tau \sim (N = 1)^{\alpha}$. The values of the scaling exponents are the slopes of the least-squares lines shown in Figure 4.

The exponent for the free-chain ($c = 0$) case is fairly close to the scaling prediction of 2.2. Up to a concentration of

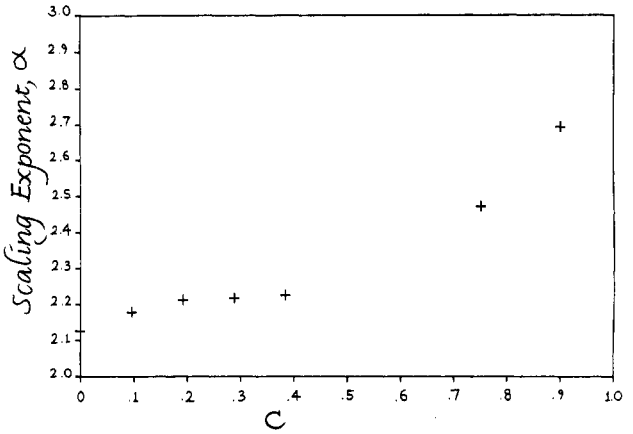

Figure 5. Plot of the relaxation time scaling exponent, α, vs. concentration, c.

0.384 the exponents increase only gradually with concentration, but there is a dramatic increase at $c = 0.750$ and $c = 0.900$. This is shown graphically in Figure 5, which is a plot of the scaling exponent, α, vs. concentration, c.

Figure 5 shows clearly that there are significant deviations from the predictions of the Rouse model as the concentration increases. The scaling exponent moves toward the value of 3.0 predicted by the reptation model, but the value of 2.70 at $c = 0.900$ is still rather far from the reptation value. The exponent seems to be increasing rapidly with concentration so it might be interesting to study systems with concentrations greater than 0.900. Simulations at concentrations greater than 0.900, however, are impractical, at least with our computational facilities. The simulation run for $N = 48$ and $c = 0.900$ required approximately 1000 of CPU time on our Hewlett-Packard 1000, series A900 computer. It is also not clear whether a lattice model simulation at concentrations much greater than 0.900 would represent a reasonable physical system since there are so few unoccupied sites.

There are very few previous studies with which to compare these results. Deutsch[13] has studied a rather dense cubic lattice system, but he only calculated monomer diffusion. Kremer's[15] elegant and careful study of the dynamics of diamond lattice chains also focused mainly on the monomer diffusion and did not look at the chain length and concentration dependence of the relaxation time. The only previous work to which these results can be directly compared is the recent paper by Kranbuehl and Verdier.[19] Kranbuehl and Verdier have simulated the dynamics of cubic lattice chains at concentrations up to $c = 0.800$ and have calculated the relaxation times as a function of chain length and concentration. They find only a weak dependence of the scaling exponent α on concentration with the exponent increasing from about 2.7 at $c = 0.1$ to about 3.0 at $c = 0.8$. The elementary motions used by Kranbuehl and Verdier, however, are quite different from the ones used here. The early work of Kranbuehl and Verdier was criticized by Deutch and co-workers[20] as having artificial constraints in the movement algorithm which overemphasize the effects of excluded volume. The more recent work of Kranbuehl and Verdier including their many-chain simulation uses a modified set of elementary motions which may answer the objections of Deutch and co-woerkers, although their value for the scaling exponent at $c = 0$ (isolated chain) differs significantly from our value and from the scaling prediction.[3] In view of the differences in behavior at $c = 0$ it is not surprising that the concentration dependence of the relaxation times is different in the Kranbuehl–Verdier simulation from that reported here. The difference is certainly due to the different elementary motions employed in the simulations. A more detailed study of the dynamics of both models is needed in order to fully understand the effect of the different elementary motions.

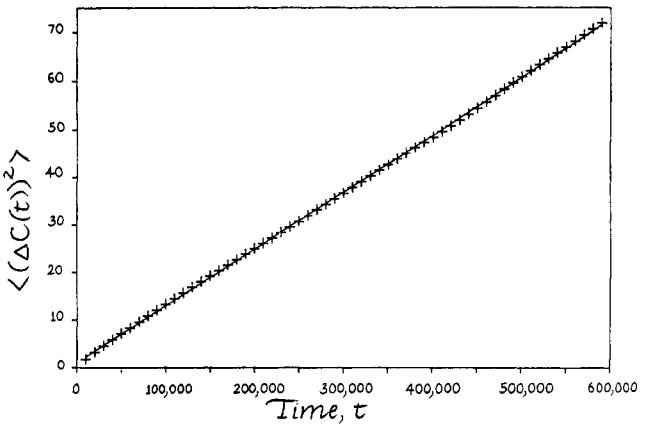

Figure 6. Plot of the mean square displacement of the center of mass, $\langle(\Delta C(t))^2\rangle$, vs. time, t for a chain of length $N = 48$ at concentration $c = 0.900$. The solid line is the least-squares line used to determine the diffusion constant.

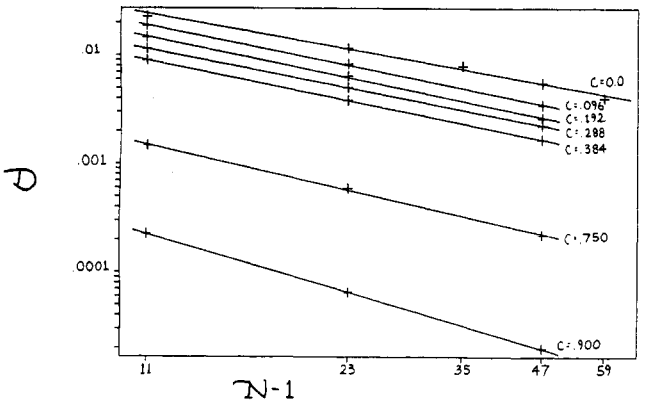

Figure 7. Double logarithmic plot of the center of mass diffusion constant, D, vs. chain length, $N - 1$, for various concentrations. The solid lines are linear least-squares fits used to determine the scaling exponents, β.

Table III
Center of Mass Diffusion Constants (D) as a Function of Chain Length (N) and Concentration (c)

	D			
c^a	12	24	48	β^b
0.000	0.022 6	0.011 7	0.005 55	1.00
0.096	0.018 6	0.008 35	0.003 49	1.15
0.192	0.014 6	0.006 46	0.002 64	1.18
0.288	0.011 4	0.005 06	0.002 25	1.12
0.384	0.008 98	0.003 86	0.001 67	1.16
0.750	0.001 47	0.000 596	0.000 222	1.30
0.900	0.000 227	0.000 065 3	0.000 019 9	1.68

[a] Units: beads per lattice site. [b] Scaling exponent for the relation $D \sim (N - 1)^{-\beta}$. The values of the scaling exponents are the slopes of the least-squares lines shown in Figure 7.

Center of Mass Diffusion Constants. Figure 6 is a typical plot of the mean square center of mass displacement $\langle(\Delta C(t)^2\rangle$ vs. time at $N = 48$ and $c = 0.900$. After a very short induction period the curve is quite linear. The least-squares line used to determine the diffusion constant is also shown. The values of the diffusion constant are collected in Table III.

Figure 7 is a scaling plot of ln D vs. ln $(N - 1)$. The least-squares lines used to estimate the exponent in the scaling relationship

$$D \sim (N - 1)^{-\beta} \quad (5)$$

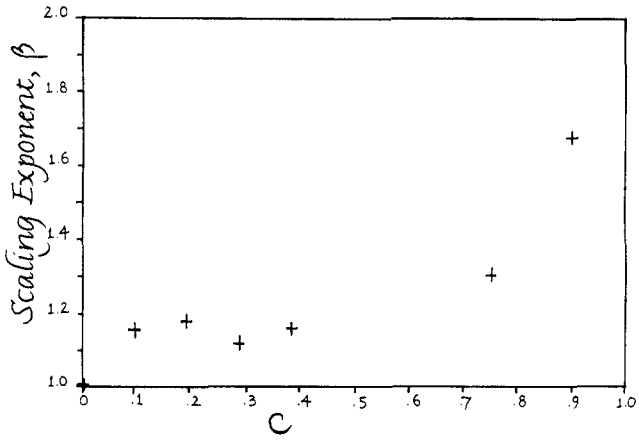

Figure 8. Plot of the diffusion constant scaling exponent, β, vs. concentration, c.

are also shown. The values of the scaling exponent are also given in Table III. The exponent for the free chain (c = 0) is fairly close to the Rouse model prediction of 1.0. As with the exponent for the relaxation time, the exponent β increases gradually with concentration up to c = 0.384, but there is a dramatic increase at c = 0.750 and c = 0.900. This is shown graphically in Figure 8, which is a plot of the scaling exponent, β, vs. concentration, c. The behavior of the exponent β with concentration is very similar to that of the exponent α. At high concentrations the exponent has moved toward the reptation model prediction of 2.0, but falls considerably short. The value at c = 0.900 is 1.69.

Again, there is very little previous work with which to compare these results. Kremer[15] did look at the center of mass diffusion but did not study the chain length or concentration dependence. Kranbuehl and Verdier[19] did compute the center of mass diffusion constants in their simulation but did not explicitly look at the scaling behavior. In view of the differences in the movement rules used a detailed comparison does not seem warranted.

The terminal relaxation time and the center of mass diffusion constant are dynamic properties that depend on large-scale motions of the chain. It seems that these large-scale motions are being affected by interchain entanglements, but that the effects are significant only at rather high concentrations. Both properties show the same type of concentration dependence. The reptation model also predicts that the shorter range motions such as the diffusion of a single monomer will also change as entanglement effects become important. We have also studied the monomer diffusion as a function of concentration and chain length to determine whether the deviations seen in the long-range properties also occur in the short-range properties.

Central Monomer Diffusion. The mean square displacement of a central monomer of a free Rouse chain[21] should have three distinct regimes of behavior over time. At very short times the mean square displacement $\langle(\Delta M(t))^2\rangle$ should be proportional to t^1. At intermediate times the displacement should vary as $t^{1/2}$ for an ideal chain or as a slightly larger power (0.59) for an expanded chain. Finally, at long times the monomer diffusion should follow the center of mass and will again be proportional to t^1. The reptation model predicts a quite different behavior in the intermediate-time region.[22] The tube constraint causes the intermediate-time ($t^{1/2}$) region to itself split into three distinct regions, an initial $t^{1/2}$ region, an intermediate $t^{1/4}$ region, and a final $t^{1/2}$ regime. The reptation prediction is shown graphically in Figure 9, which is a schematic double logarithmic plot of the displacement vs. time.

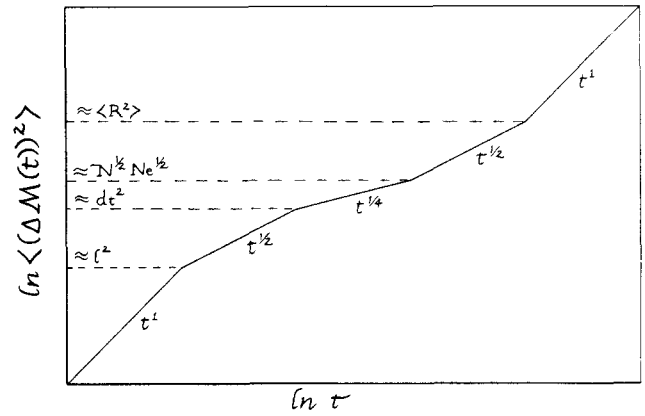

Figure 9. Schematic representation of the mean square monomer displacement $\langle(\Delta M(t))^2\rangle$ as a function of time as predicted by the theory of reptation. On the left-hand side are shown the approximate displacements at which the different regions of behavior occur. l is the bond length, d_t is the tube diameter, N_e is the chain length between entanglements, N is the chain length, and $\langle R^2\rangle$ is the mean square end-to-end distance.

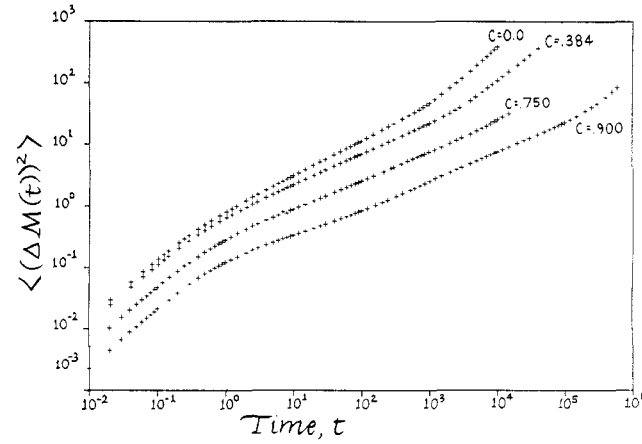

Figure 10. Double logarithmic plot of the mean square monomer displacement $\langle(\Delta M(t))^2\rangle$ vs. time, t, for chains of length N = 48 at various concentrations.

There should be five distinct regions of behavior, as illustrated.

The monomer diffusion for chains of length N = 48 at several concentrations is shown on a double logarithmic plot of Figure 10. The free-chain (c = 0) curve shows typical Rouse-like behavior for an expanded chain. As the concentration increases to 0.384, the behavior is still Rouse-like, but the intermediate-time region has flattened out slightly to a slope of nearly $^1/_2$. When the concentration has increased to 0.900, a distinct inflection or hump in the curve has developed at the short-time end of the intermediate-time regime. This is a clear deviation from the Rouse-like behavior seen at lower concentrations, but does not conform to the reptation prediction. There are two differences. First, this hump or inflection is merely that and does seem to be a clear combination of a $t^{1/2}$ and $t^{1/4}$ region. In fact, its slope is approximately $^3/_8$. Second, the inflection occurs at very small displacements (ca. 10^{-1}) and therefore does not seem to be due to a tube constraint on the monomer motion.

This same feature occurs at c = 0.900 for all chain lengths studied. This is seen in Figure 11, which is a double logarithmic plot of ln $\langle(\Delta M(t))^2\rangle$ vs. ln t for chain lengths N = 12, 24, and 48 all at c = 0.900. The position of the inflection seems to be independent of the chain length since the curves almost superimpose up to the point where the center of mass diffusion begins to dominate the monomer displacement.

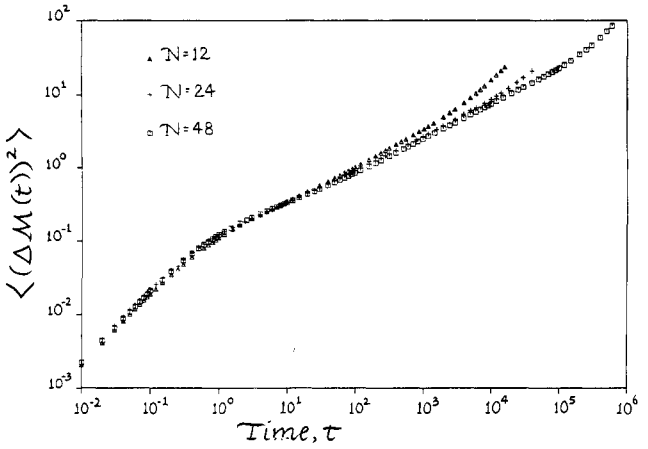

Figure 11. Double logarithmic plot of the mean square monomer displacement, $\langle(\Delta M(t))^2\rangle$, vs. time, t, for various chain lengths at $c = 0.900$.

As with the two other dynamic properties there is a clear deviation from Rouse-like behavior in the monomer diffusion at high concentrations. There are two previous lattice model simulations with which these results should be compared. Deutsch[13] studied the monomer diffusion of a cubic lattice chain at a concentration of about 0.72 and found a clear $t^{1/4}$ region in agreement with the theory of reptation. Unfortunately Deutsch's simulation algorithm treates the inter- and intramolecular excluded volume differently. In Deutsch's model a chain is allowed to intersect itself with a certain nonzero probability. This probably favors motion along the chain contour and artificially builds in the reptation-like motion.[23] Our algorithm allows no chain overlaps at all. Since, we do not see the same behavior as Deutsch, it is clear that his results are due to this special feature in his model.

Kremer[15] studied the monomer displacement of long ($N = 200$) diamond lattice chains at $c = 0.344$ and saw only Rouse-like behavior if all chains were mobile. He did see a $t^{1/4}$ region of all chains but one were frozen in position. Since we see no deviation from Rouse-like behavior at $c = 0.384$, our results are consistent with Kremer's in the low-concentration region. Kremer did not study higher concentrations, so no comparison can be made concerning concentration dependence of the monomer diffusion.

Conclusions

The results presented above show that significant deviations from the Rouse model are observed in multiple-chain cubic lattice systems if the concentration is large enough. It seems clear that the chain motions are being affected by entanglements, but even at the highest concentration studied ($c = 0.900$) the results do not agree with the reptation theory. Since the chains studied were rather short, the lack of agreement with reptation is perhaps not surprising. Any general theory of entanglement effects will have to explain the change in the scaling behavior as a function of concentration and chain length between the Rouse regime and the reptation regime.

One obvious possible explanation for the results obtained here involves the relative success of the normal-bead and crankshaft motions as a function of concentration. The original Verdier–Stockmayer model which included only the normal-bead motion had an N^3 time scale for the terminal relaxation time in the presence of excluded volume. Since the two-bead crankshaft motion requires two adjacent open sites to be successful, it will be selectively suppressed as the concentration increases. As the two-bead motions disappear, the scaling exponent should increase. We are in the process of investigating this effect in detail by arbitrarily reducing the probability of success of the two-band motion. Preliminary results on the terminal relaxation time and the center of mass diffusion show that suppression of the crankshaft can account for about half of the observed deviation from Rouse-like behavior, but far from all of the deviation.[24] It seems that longer range entanglements are also important. Full details will be published in the near future.[24]

In this paper we have studied only the three simplest dynamic properties. It would be interesting to see how the deviations from the Rouse theory appear in the higher order normal modes. This analysis is also in progress. In that way we hope to study the entanglement effects more deeply. Perhaps these simple computer simulation studies can provide some insight into the detailed nature of entanglement effects in polymer dynamics.

Acknowledgment. We thank the Research Corp. and the ARCO Foundation for financial support. We also thank the University of Tennessee Computer Center for their support and patience. The Hewlett-Packard 1000 series A900 computer was purchased with funds provided by the National Science Foundation, the Department of Energy, the Research Corp., and the University of Tennessee Research Incentive Program.

References and Notes

(1) H. Yamakama, "Modern Theory of Polymer Solution", Harper and Row, New York, 1971, Chapter 6.
(2) P. G. DeGennes, *J. Chem. Phys.*, **55**, 572 (1971).
(3) P. G. DeGennes, "Scaling Concepts in Polymer Physics", Cornell University Press, Ithaca, NY, 1979.
(4) M. Doi and S. F. Edwards, *J. Chem. Soc., Faraday Trans. 2*, **74**, 1789, 1802, 1818 (1978).
(5) J. D. Hoffman, *Polymer*, **23**, 656 (1982).
(6) Y. H. Kim and R. P. Wool, *Macromolecules*, **16**, 1115 (1983).
(7) T. J. Tulig and M. Tirrell, *Macromolecules*, **14**, 1501 (1981); **15**, 459 (1982).
(8) W. W. Greassley, *Adv. Polym. Sci.*, **47**, 67 (1982).
(9) P. G. DeGennes and L. Leger, *Ann. Rev. Phys. Chem.*, **33**, 49 (1982).
(10) D. Richter, A. Baumgärtner, K. Binder, B. Ewen, and J. B. Hayter, *Phys. Rev. Lett.*, **47**, 109 (1981).
(11) A Baumgärtner and K. Binder, *J. Chem. Phys.*, **75**, 2994 (1981).
(12) M. Bishop, D. Ceperley, H. L. Frisch, and M. H. Kalos, *J. Chem. Phys.*, **76**, 1557 (1982).
(13) J. M. Deutsch, *Phys. Rev. Lett.*, **49**, 926 (1982).
(14) K. E. Evans and S. F. Edwards, *J. Chem. Soc., Faraday Trans. 2*, **77**, 1891 (1981).
(15) K. Kremer, *Macromolecules*, **16**, 1632 (1983).
(16) M. T. Gurler, C. C., Crabb, D. M. Dahlin, and J. Kovac, *Macromolecules*, **16**, 398 (1983).
(17) M. Dial, K. S. Crabb, C. C. Crabb, and J. Kovac, *Macromolecules*, in press.
(18) M. Bishop, M. H. Kalos, A. D. Sokal, and H. L. Frisch, *J. Chem. Phys.*, **79**, 3496 (1983), and references therein.
(19) D. E. Kranbuehl and P. H. Verdier, *Macromolecules*, **17**, 749 (1984).
(20) H. J. Hilhorst and J. M. Deutch, *J. Chem. Phys.*, **63**, k153 (1975); H. Boots and J. M. Deutch, *J. Chem. Phys.*, **67**, 4608 (1977).
(21) P. G. DeGennes, *Physics*, **3**, 37 (1967).
(22) P. G. DeGennes, *J. Chem. Phys.*, **72**, 4756 (1980).
(23) K. Kremer, *Phys. Rev. Lett.*, **51**, 1923 (1983). For a response see J. M. Deutsch, *Phys. Rev. Lett.*, **51**, 1924 (1983).
(24) C. Stokely, C. C. Crabb, and J. Kovac, to be submitted for publication.
(25) C. Domb, *J. Chem. Phys.*, **38**, 2957 (1963).